LGALS3BP in Microglia Promotes Retinal Angiogenesis Through PI3K/AKT Pathway During Hypoxia

Chenyang Zhao,[1–3] Yusen Liu,[1–3] Jiayu Meng,[1–3] Xiaotang Wang,[1–3] Xianyang Liu,[1–3] Wanqian Li,[1–3] Qian Zhou,[1–3] Junjie Xiang,[1–3] Na Li,[4] and Shengping Hou[1–3]

[1]The First Affiliated Hospital of Chongqing Medical University, Chongqing, China
[2]Chongqing Key Laboratory of Ophthalmology, Chongqing, China
[3]Chongqing Branch of National Clinical Research Center for Ocular Diseases, Chongqing, China
[4]College of Basic Medicine, Chongqing Medical University, Chongqing, China

Correspondence: Shengping Hou, The First Affiliated Hospital of Chongqing Medical University, 1 Yixueyuan Road, Yuzhong District, Chongqing 400016, China; sphou828@163.com.
Na Li, College of Basic Medicine, Chongqing Medical University, 1 Yixueyuan Road, Yuzhong District, Chongqing 400016, China; coco0411@126.com.

CZ and YL contributed equally to this work.

Received: March 30, 2022
Accepted: July 2, 2022
Published: July 27, 2022

Citation: Zhao C, Liu Y, Meng J, et al. LGALS3BP in microglia promotes retinal angiogenesis through PI3K/AKT pathway during hypoxia. *Invest Ophthalmol Vis Sci.* 2022;63(8):25. https://doi.org/10.1167/iovs.63.8.25

Purpose. Retinal microglia promote angiogenesis and vasculopathy in oxygen-induced retinopathy (OIR); however, its specific molecular mechanism in the formation of retinal angiogenesis remains unclear. The lectin galactoside-binding soluble 3 binding protein (LGALS3BP), a member of the scavenger receptor cysteine-rich (SRCR) domain protein family, is involved in tumor neovascularization, and we therefore hypothesized that LGALS3BP plays an active role in microglia-induced angiogenesis.

Methods. The expression of LGALS3BP in microglia was detected by immunofluorescence, RT-qPCR, and western blotting. Functional assays of human umbilical vein endothelial cells (HUVECs) such as migration, proliferation, and tube formation were measured by Transwell, EdU, and Matrigel assays. Angiogenesis-related factors and PI3K/AKT levels were detected by western blotting. The relationship between LGALS3BP and PI3K or HIF-1α was investigated by immunoprecipitation.

Results. Our results showed that the expression of LGALS3BP was significantly increased in microglia surrounding neovascularization of the OIR mice and was also upregulated in human microglial clone 3 (HMC3) cells after hypoxia. Moreover, HUVECs co-cultured with hypoxic HMC3 cells showed increased migration, proliferation, and tube formation, as well as levels of angiogenesis-related factor. However, the proangiogenic ability and angiogenesis-related factor expression of HMC3 cells was suppressed after silencing LGALS3BP. LGALS3BP induces the upregulation of angiogenesis-related factors through the PI3K/AKT pathway and then promotes angiogenesis in microglia.

Conclusions. Collectively, our findings suggest that LGALS3BP in microglia plays an important role in angiogenesis, suggesting a potential therapeutic target of LGALS3BP for angiogenesis.

Keywords: LGALS3BP, microglia, angiogenesis, angiogenic factors

Retinopathy of prematurity (ROP) usually occurs in preterm infants who receive supplemental oxygen therapy to regain normoxic conditions, and lower birth weight preterm infants tend to be associated with higher morbidity.[1] Currently, ROP is the leading cause of childhood blindness worldwide.[2] So far, the treatment methods for ROP mainly include laser ablation of the avascular retina and anti-vascular endothelial growth factor (VEGF) therapy in the vitreous cavity.[3,4] However, compared with term infants, the sequelae of these two treatments for premature infants are obvious: refractive error and glaucoma.[5] Therefore, there is an urgent need to find new potential molecular therapeutic targets to inhibit abnormal vascular proliferation of ROP.

Microglia have been extensively studied as retinal innate immune cells, especially in inflammation-related disease models.[6,7] In recent years, more and more studies have reported that microglia are also associated with blood vessel formation in addition to classical biological functions such as pruning, phagocytosis, and monitoring neuronal activity.[8,9] Checchin et al.[10] found that, during retinal development, all vascular endothelial cells appear to be closely associated with microglia, and microglia turn vascular sprouts in the deep plexus into superficial vascular plexus, increasing the branch density of the superficial retinal vascular plexus.[11,12] Meanwhile, some parenchymal microglia in mammalian brain tissues (juxtavascular microglia) directly contact the basal lamina of blood vessels. Overall, there is a dynamic and ongoing interaction between microglia and microvessels.[13]

Lectin galactoside-binding soluble 3 binding protein (LGALS3BP, also known as 90K or Mac-2BP), a member of the scavenger receptor cysteine-rich (SRCR) domain protein family,[14,15] is a ubiquitous multifunctional secreted glycoprotein involved in immunity and inflammation that was originally studied in the context of tumor transformation

and cancer progression.[16,17] Immunohistochemical and gene expression analyses have shown significantly higher levels of LGALS3BP in different types of human malignancies[18]; moreover, it has been shown to be correlated with the prognosis and survival of cancer patients.[19]

Recent studies have reported that upregulated LGALS3BP promotes tumor growth and angiogenesis by increasing vascular endothelial growth factor A (VEGF-A) expression.[17,20] However, its proangiogenic properties in microglia during retinal angiogenesis have not been investigated. In our study, we showed that LGALS3BP in microglia plays an important role in promoting angiogenesis. Mechanically, LGALS3BP upregulates the expression of angiogenesis-related factors in microglia by activating the phosphatidylinositol 3-kinase (PI3K)/protein kinase B (AKT) signaling pathway and then promotes tube formation of human umbilical vein endothelial cells (HUVECs).

Materials and Methods

Animals and OIR Model Establishment

C57BL/6J mice were provided by the Experimental Animal Center of Chongqing Medical University and were housed in a specific pathogen-free facility in compliance with the ARVO Statement for the Use of Animals in Ophthalmic and Vision Research. To establish a mouse oxygen-induced retinopathy (OIR) model, 7-day-old pups were kept in an incubator with an oxygen concentration of 75% ± 2% for 5 days, then transferred to room air for 5 days. Control mice were placed in room air for 17 days. On the 17th day, two groups of mice were euthanized, the eyeballs were taken out, and the retinas were separated for immunofluorescence, western blotting, and PCR.

Cell Culture and Hypoxic Exposure

The human microglial clone 3 (HMC3) cell line was purchased from FuHeng Biology (Shanghai, China) and cultured in Gibco Minimum Essential Medium (MEM; Thermo Fisher Scientific, Waltham, MA, USA) containing 10% Gibco fetal bovine serum (FBS; Thermo Fisher Scientific), 100 µg/mL streptomycin, and 100 µg/mL penicillin in a humidified atmosphere with 5% CO_2 at 37°C. HUVECs were obtained from FuHeng Biology (Shanghai, China) and cultured in Dulbecco's modified Eagle's medium (DMEM; Thermo Fisher Scientific) containing 10% FBS, 100 µg/mL streptomycin, and 100 µg/mL penicillin in a humidified atmosphere with 5% CO_2 at 37°C. Hypoxic culture conditions were achieved with a multi-gas incubator (Thermo Fisher Scientific) containing a gas mixture composed of 94% N_2, 5% CO_2, and 1% O_2. The cells were cultured in MEM for the indicated time.[21–23]

Reagents

Antibody against ionized calcium binding adaptor molecule 1 (IBA-1; 01919741, 1:1000) was purchased from Wako (Richmond, VA, USA). Antibodies (1:1000) purchased from Abcam (Cambridge, UK) included Recombinant Anti-LGALS3BP antibody [EPR21757-33] (rabbit monoclonal to LGALS3BP, ab217572), Anti-LGALS3BP antibody [OTI3D6] (mouse monoclonal to LGALS3BP, ab236509), Recombinant Anti-Matrix Metalloproteinase-2 (MMP-2) antibody [EPR17003-25] (rabbit monoclonal to MMP-2, ab181286), Recombinant Anti-MMP-9 antibody [EPR22140-154] (rabbit monoclonal to MMP-9, ab228402), Anti–Hypoxia-Inducible Factor 1 alpha (HIF-1α) antibody (rabbit polyclonal antibody to HIF-1 alpha, ab216842), Anti-VEGFA antibody (rabbit polyclonal to VEGFA, ab46154), Anti-CD31 antibody [JC/70A] (mouse monoclonal to CD31, ab9498), and Anti-Occludin antibody [CL1555] (mouse monoclonal to occludin, ab242202). Antibody against HIF-1α (mouse monoclonal antibody for immunofluorescence, 66730-1-lg; 1:1000) was obtained from Proteintech (Shanghai, China). Antibodies obtained from Affinity Biosciences (1:000; Cincinnati, OH, USA) included P-PI3K (AF3241), PI3K (AF6241), P-AKT (AF0016), and AKT (AF6261). PI3K inhibitor LY294002 was procured from TargetMol (Boston, MA, USA). β-actin (20536-1-AP; 1:000) and zona occludens 1 (ZO-1; 21773-1-AP; 1:1000) were obtained from Proteintech. Secondary antibodies were purchased from Beyotime (Shanghai, China), including goat anti-rabbit IgG (H+L), goat anti-mouse IgG (H+L), Cy3-Labeled Goat Anti-Mouse IgG (H+L), and 488-Labeled Goat Anti-Rabbit IgG (H+L). RT Master Mix and SYBR Green qPCR Master Mix (Low ROX) for PCR were purchased from MedChemExpress (Shanghai, China).

Immunofluorescence

HMC3 cells were fixed with 4% paraformaldehyde for 15 minutes, followed by permeabilization with 0.5% Triton X-100 for 20 minutes. Then, antigen was blocked with goat serum for 30 minutes and incubated with the anti-HIF-1α antibody at 4°C overnight. On the next day, cells were washed with PBS three times and incubated with Cy3-Labeled Goat Anti-Rabbit IgG (H+L) for 30 minutes at room temperature in the dark. Finally, nuclei of these cells were stained with 4′,6-diamidino-2-phenylindole (DAPI), and images were collected using a microscope (Leica, Wetzlar, Germany).

Mice were anesthetized with 4% sodium pentobarbital, followed by intracardial perfusion with 0.1-M PBS (pH 7.4) containing 150 U/mL heparin and infusion with 4% paraformaldehyde in 0.1-M phosphate buffer. The mice eyeballs were taken out and placed in 4% paraformaldehyde for 2 hours at room temperature. The cornea and lens were removed to obtain the retinas, which were cut into a four-leaf clover shape and transferred to a glass slide. The cell membrane was permeabilized with 0.5% Triton X-100 for 15 minutes, and then antigen was blocked with goat serum for 30 minutes at 37°C. The retinas were then incubated with diluted primary antibody overnight at 4°C followed by incubation with the secondary antibody at 37°C for 1 hour. The procedure of section staining is similar to that of retinal staining, except that DAPI is added at the end. Immunofluorescence was visualized using a Leica confocal microscope).

Western Blotting

Tissues or cells were lysed by radio immunoprecipitation assay (RIPA; Beyotime) with a lysis buffer containing 1% phenylmethanesulfonyl fluoride (Beyotime). Protein concentration was detected using a bicinchoninic acid assay quantification kit (Beyotime). The same quantities of protein samples were electrophoresed with 10% sodium dodecyl sulfate (SDS) polyacrylamide gel and then transferred onto 0.45-mm polyvinylidene difluoride membranes

Investigative Ophthalmology & Visual Science

(MilliporeSigma, Billerica, MA, USA). After blocking with 5% nonfat dry milk for 2 hours at room temperature, the membrane was incubated with primary antibody for immunoblotting at 4°C overnight. Membranes were incubated with secondary antibody for 1 hour at room temperature. Protein band signals were detected with an ECL kit (Mengbio, Chongqing, China). Band density was quantified using ImageJ (National Institutes of Health, Bethesda, MD, USA) and normalized to β-actin.

Real-Time Quantitative PCR

RNA from cells or tissues was extracted by TRIzol reagent (Roche, Basel, Switzerland), and RNA concentrations were detected by spectrophotometer (Thermo Fisher Scientific). RNA was reverse transcribed to cDNA using RT Master Mix (MCE, Shanghai, China). RT-qPCR was performed using the ABI 7500 Real-Time PCR System (Applied Biosystems, Foster City, CA, USA) with SYBR Green qPCR Master Mix (MedChemExpress, Shanghai, China). All primers were synthesized by Shanghai Sangon Co., Ltd. (Shanghai, China).

Cell Migration

Migration assays were performed in 24-well modified Boyden chambers (Transwell; Corning, Inc., Corning, NY, USA) with the two compartments separated by a polycarbonate filter with an 8-mm pore size. HUVECs were placed in the upper chambers, and HMC3 cells that had been maintained under hypoxic conditions for 24 hours were seeded in the lower chambers. The chambers were incubated at 37°C and 5% CO_2 for 24 hours. The cells migrating through the filter were fixed by 4% paraformaldehyde for 10 minutes and stained with 1% crystal violet in methanol. The non-migrated cells on the upper surface of the microporous membrane were wiped away with a cotton swab, and the migrated cells on the lower surface of the microporous membrane were imaged using a Leica microscope. The migrated cells were imaged and quantified using ImageJ.

Tube Formation Assays

HUVECs were seeded into the lower chambers of 24-well Transwell plates (0.44 µm; Corning, Inc.), and HMC3 cells were cultured for 24 hours under hypoxic conditions and seeded into the upper chambers. After 24 hours of co-culture, endothelial cells were seeded into 96-well plates containing BD Matrigel (BD Biosciences, Bedford, MA, USA). Pictures were captured by an inverted microscope after 6 hours. Tube length was calculated using ImageJ and normalized to the control group.

5′-Ethynyl-2′-Deoxyuridine Assay

Cells were seeded according to the method of tube formation assays. After 24 hours of co-culture, endothelial cells were exposed to 20 µL 5′-ethynyl-2′-deoxyuridine (EdU; Beyotime) for 2 hours at 37°C. Cells were fixed with 4% paraformaldehyde for 15 minutes, and membranes were then permeabilized with 0.3% Triton X-100 (Beyotime) for another 15 minutes. Cells were incubated with a click reaction mixture for 30 minutes at room temperature in the dark and then stained with Hoechst 33342 for 10 minutes. Pictures were captured using a Leica fluorescence microscope.

Immunoprecipitation

Proteins in HMC3 cells after hypoxia were isolated with RIPA lysis buffer (ab206996, Abcam) containing protease inhibitor cocktail, and the concentration was detected based on western blotting methods. After overnight incubation with anti-LGALS3BP antibody (Proteintech) or IgG isotype control (Beyotime) at 4°C, protein complexes were adsorbed on protein A/G agarose beads (ab206996, Abcam) and eluted with SDS-PAGE loading buffer. Finally, the eluted proteins were detected by western blotting.

Statistical Analysis

All experiments were performed with least three independent replicates. All data are shown as mean ± SD, and statistical analyses were performed using SPSS Statistics 20.0 (IBM Corp., Chicago, IL, USA) and Prism 8.0 (GraphPad, San Diego, CA, USA). Unpaired Student's *t*-tests were applied to assess significance between two groups, and one-way ANOVA was applied for analyses among multiple groups. A value of $P < 0.05$ was considered statistically significant.

Results

Increased *lgals3bp* Expression in Microglia Surrounding Retinal Neovascular in the OIR Model

First, immunofluorescence staining in the retinas of OIR and control mice was performed to verify that microglia were involved in the formation of retinal neovascularization in OIR mice. More microglia near retinal neovascularization were found in OIR model mice as compared with control mice (Fig. 1A). We next co-stained LGALS3BP and IBA-1 in retinal sections from OIR and control mice. As shown in our results, LGALS3BP was expressed at lower levels in the retinas of control mice with faint staining, but the staining in IBA-1 positive cells of the OIR mice was clearer (Fig. 1B). Then, we detected the *lgals3bp* mRNA and protein levels in the retinas of OIR mice and control mice. Compared with control mice, both mRNA and protein levels of LGALS3BP in OIR mice were significantly increased. Also, the expression of HIF-1α was increased, which was consistent with the change in LGALS3BP expression (Figs. 1C, 1D).

Increased Expression of LGALS3BP in HMC3 Cells Induced by Hypoxia

We used HMC3 cells (a microglia cell line) to detect the expression of LGALS3BP under physical hypoxic conditions. Our results showed that LGALS3BP mRNA and protein levels were significantly increased after hypoxia in HMC3 cells, and HIF-1α expression was significantly upregulated after hypoxia. (Figs. 2A–2C). We co-cultured HMC3 cells with HUVECs to explore changes in the tube-formation ability of HUVECs. Compared with the control group, hypoxic HMC3 cells increased the Matrigel-based tube-formation ability of HUVECs (Fig. 2D).

Investigative Ophthalmology & Visual Science

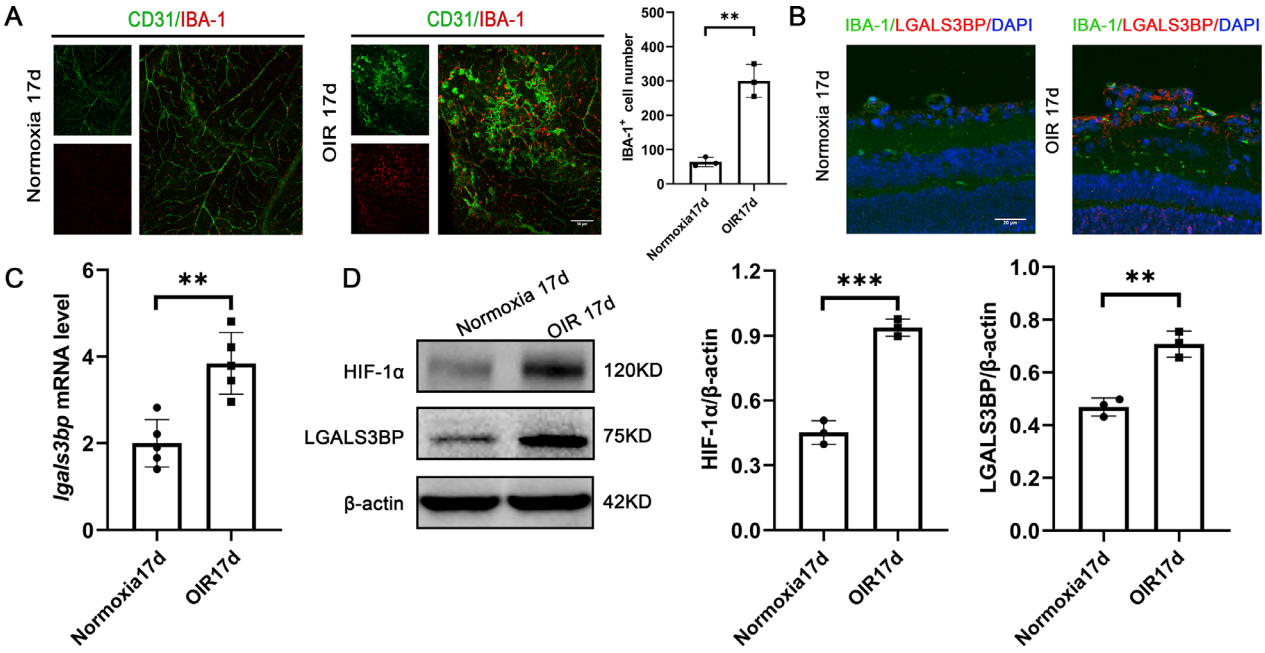

Figure 1. Increased expression of LGALS3BP was positively correlated with angiogenesis in the OIR retinas. (**A**) Immunofluorescence images of retinal flatmounts in normoxia mice and OIR mice stained with IBA-1 (microglia marker) and CD31 (endothelial cell maker), with quantification of IBA-1$^+$ cell numbers on the *right* (mean ± SD; n = 3/group; $^{**}P < 0.01$, unpaired Student's t-test). *Scale bars*: 50 µm. (**B**) Representative immunofluorescence images of IBA-1 and LGALS3BP in the retinas of normoxia and OIR mice. *Scale bars*: 20 µm. (**C**) mRNA level of *lgals3bp* in the OIR retinas (mean ± SD; n = 5/group; $^{**}P < 0.01$, unpaired Student's t-test). (**D**) Protein expression of HIF-1α and LGALS3BP in OIR retinas (mean ± SD; n = 3/group; $^{**}P < 0.01$, $^{***}P < 0.001$, unpaired Student's t-test).

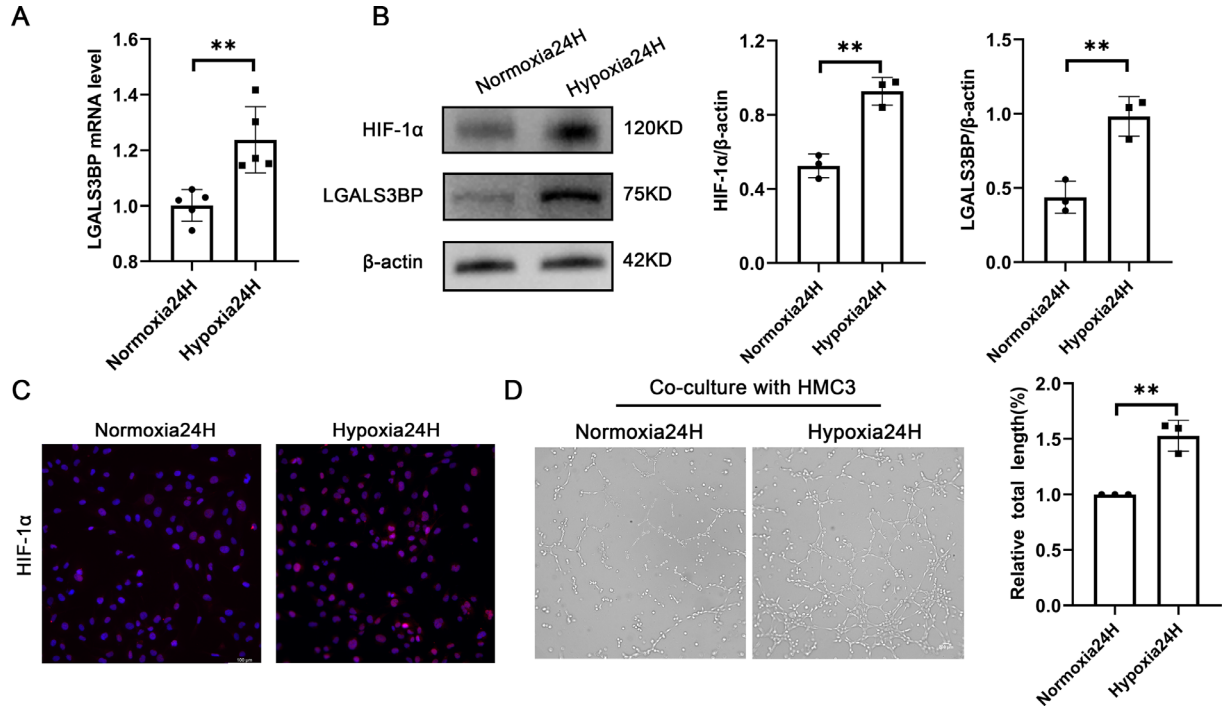

Figure 2. Hypoxia upregulated LGALS3BP and HIF-1α expression in in vitro HMC3 cells. (**A**) mRNA expression of LGALS3BP in hypoxic HMC3 cells (mean ± SD; n = 5/group; $^{**}P < 0.01$, unpaired Student's t-test). (**B**) Representative western blotting images and quantitative analysis of the protein expression of LGALS3BP and HIF-1α in HMC3 cells under hypoxia for 24 hours (mean ± SD; n = 3/group; $^{**}P < 0.01$, unpaired Student's t-test). (**C**) Representative immunofluorescence images of HIF-1α in HMC3 cells after 24 hours of hypoxia. *Scale bar*: 100 µm. (**D**) Representative HUVEC images and quantification of in vitro tube-formation analysis in Matrigel (mean ± SD; n = 3/group; $^{**}P < 0.01$, unpaired Student's t-test). *Scale bars*: 200 µm.

Investigative Ophthalmology & Visual Science

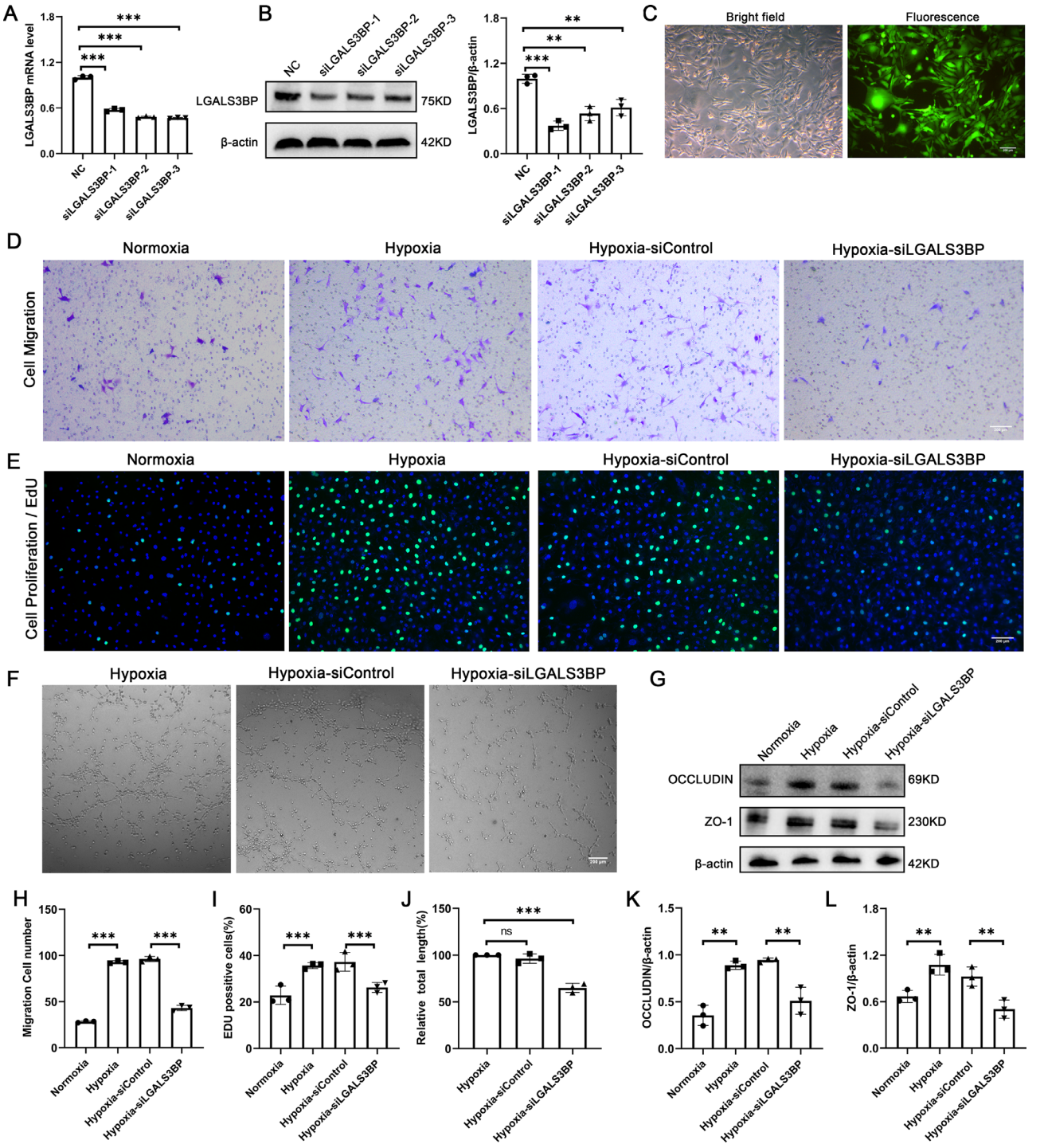

Figure 3. Effects of RNA silencing of LGALS3BP on HUVEC-related phenotypes. (**A**, **B**) mRNA and protein levels of LGALS3BP in HMC3 cells after transfection with negative control (NC), siLGALS3BP-1, siLGALS3BP-2, or siLGALS3BP-3 virus (mean ± SD; $n = 3$/group; $^{**}P < 0.01$, $^{***}P < 0.001$, one-way ANOVA). (**C**) Images of siLGALS3BP-1 transfected HMC3 cells under white light and fluorescence. *Scale bars*: 200 µm. (**D**, **H**) Transwell migration assay of HUVECs after co-culture with LGALS3BP-silent HMC3 cells (mean ± SD; $n = 3$/group; $^{***}P < 0.001$, one-way ANOVA). *Scale bars*: 200 µm. (**E**, **I**) The EdU assay was used to analyze the proliferation of HUVECs after co-culture with LGALS3BP-silent HMC3 cells (mean ± SD; $n = 3$/group; $^{***}P < 0.001$, unpaired Student's *t*-test). *Scale bars*: 200 µm. (**F**, **J**) Representative images and quantification of in vitro tube formation analysis in Matrigel (mean ± SD; $n = 3$/group; $^{ns}P > 0.05$, $^{***}P < 0.001$, one-way ANOVA). *Scale bars*: 200 µm. (**G**, **K**, **L**) Quantitative analysis of the protein expression of occludin and ZO-1 in HUVECs after co-culture with LGALS3BP-silent HMC3 cells (mean ± SD; $n = 3$/group; $^{**}P < 0.01$, one-way ANOVA).

Investigative Ophthalmology & Visual Science

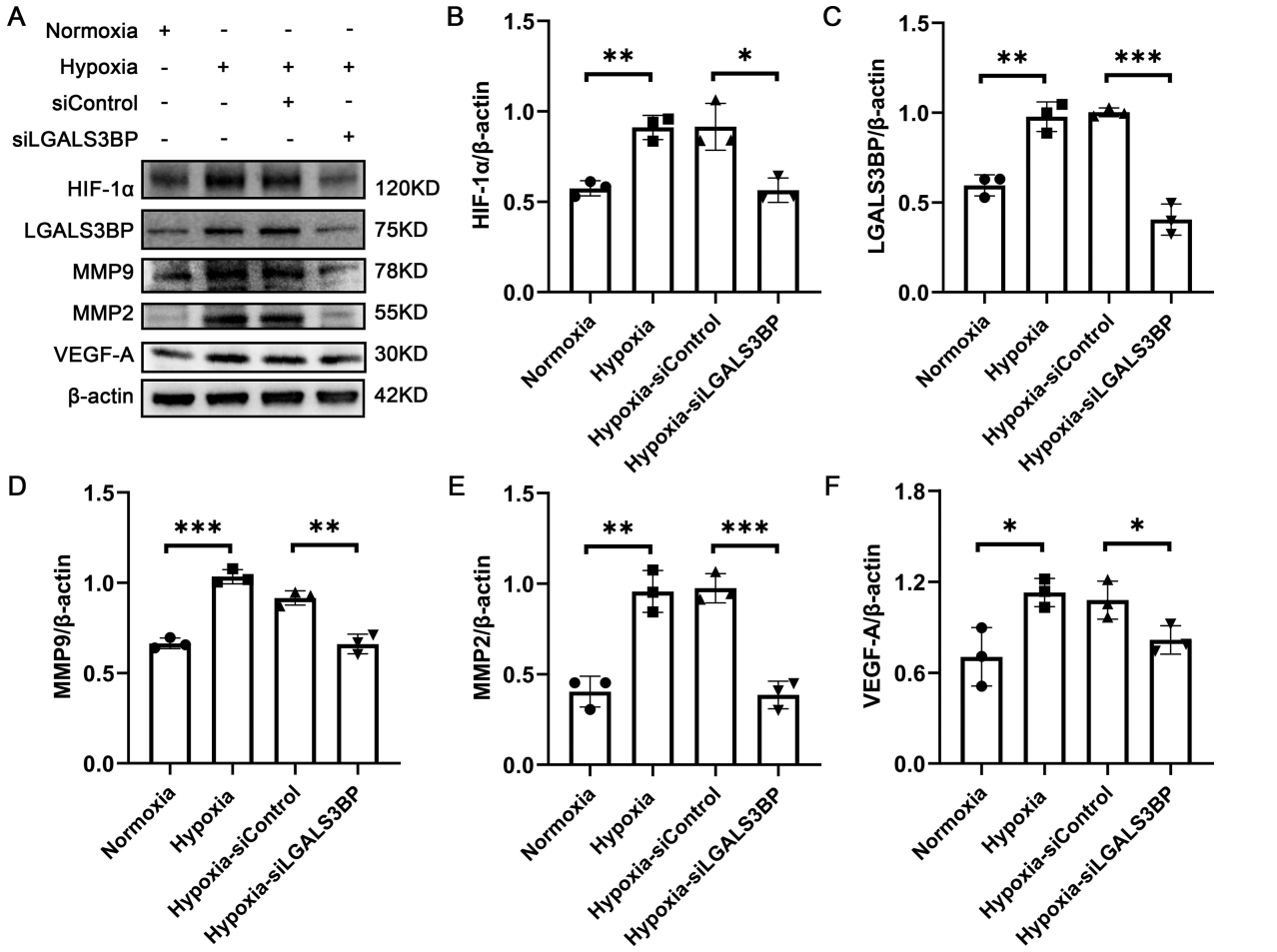

Figure 4. Silencing of LGALS3BP inhibits the expression of angiogenesis-related factors. (**A**) Representative western blotting images of HIF-1α, LGALS3BP, MMP-9, MMP-2, and VEGF-A in LGALS3BP-silent HMC3. (**B–F**) Quantification of the relative fold changes of these proteins (mean ± SD; $n = 3$/group; $^{*}P < 0.05$, $^{**}P < 0.01$, $^{***}P < 0.001$, one-way ANOVA).

Silencing of LGAS3BP in HMC3 Cells Inhibits the Migration, Proliferation, and Tube Formation of HUVECs

To investigate the role of LGALS3BP in HMC3 cells with regard to HUVEC-related functions, we first used three candidate LGALS3BP lentiviruses to silence LGALS3BP in HMC3 cells. Approximately 50% silent efficiency for LGALS3BP was detected in HMC3 cells (Figs. 3A, 3B). Based on comprehensive comparisons, the lentiviral siLGALS3BP-1 demonstrated the highest knockdown efficiency and was chosen to transfect the HMC3 cell line. Our results indicated approximately 90% transfection efficiency in HMC3 cells after transfection (Fig. 3C). Next, we investigated the effects of LGALS3BP silence in HMC3 cells on HUVEC migration and proliferation, as well as angiogenesis. Our results showed that the migration ability of HUVECs co-cultured with hypoxia-treated HMC3 cells was significantly enhanced compared with normoxia HMC3 cells. In contrast, the migration ability of HUVECs co-cultured with hypoxia-treated and LGALS3BP-silent HMC3 cells was weaker than that in hypoxia-treated LGALS3BP-nonsilent HMC3 cells (Figs. 3D, 3H). Because our results indicated increased neovascularization of retinal flat mounts in OIR mice compared with control mice (Fig. 1A), we next evaluated the proliferative and tube formation of HUVECs. We observed that the proliferation of HUVECs co-cultured with hypoxia-treated HMC3 cells was increased, but, when LGALS3BP was silenced in HMC3 cells, the proliferation and tube-formation ability of HUVECs were significantly reduced compared with the siControl group (Figs. 3E, 3F, 3I, 3J). Previous studies have reported that occludin acts as a marker of vascular endothelial cell tube-forming activity,[24] so we also determined HUVEC expression of occludin and ZO-1 in our co-culture system. Increased expression of occludin and ZO-1 was found in HUVECs co-cultured with hypoxia-treated HMC3 cells; however, decreased expression of occludin and ZO-1 was found in HUVECs co-cultured with hypoxia-treated and LGALS3BP-silent HMC3 cells (Figs. 3G, 3K, 3L). Collectively, these results suggest that LGALS3BP in HMC3 cells plays an important role in promoting HUVEC tube formation.

Silencing LGALS3BP Inhibits the Expression of Angiogenic Factors in HMC3 Cells

To explore how LGALS3BP affects HUVEC tube formation, we examined the expression levels of several angiogenic factors in HMC3 cells. First, we found that the expression

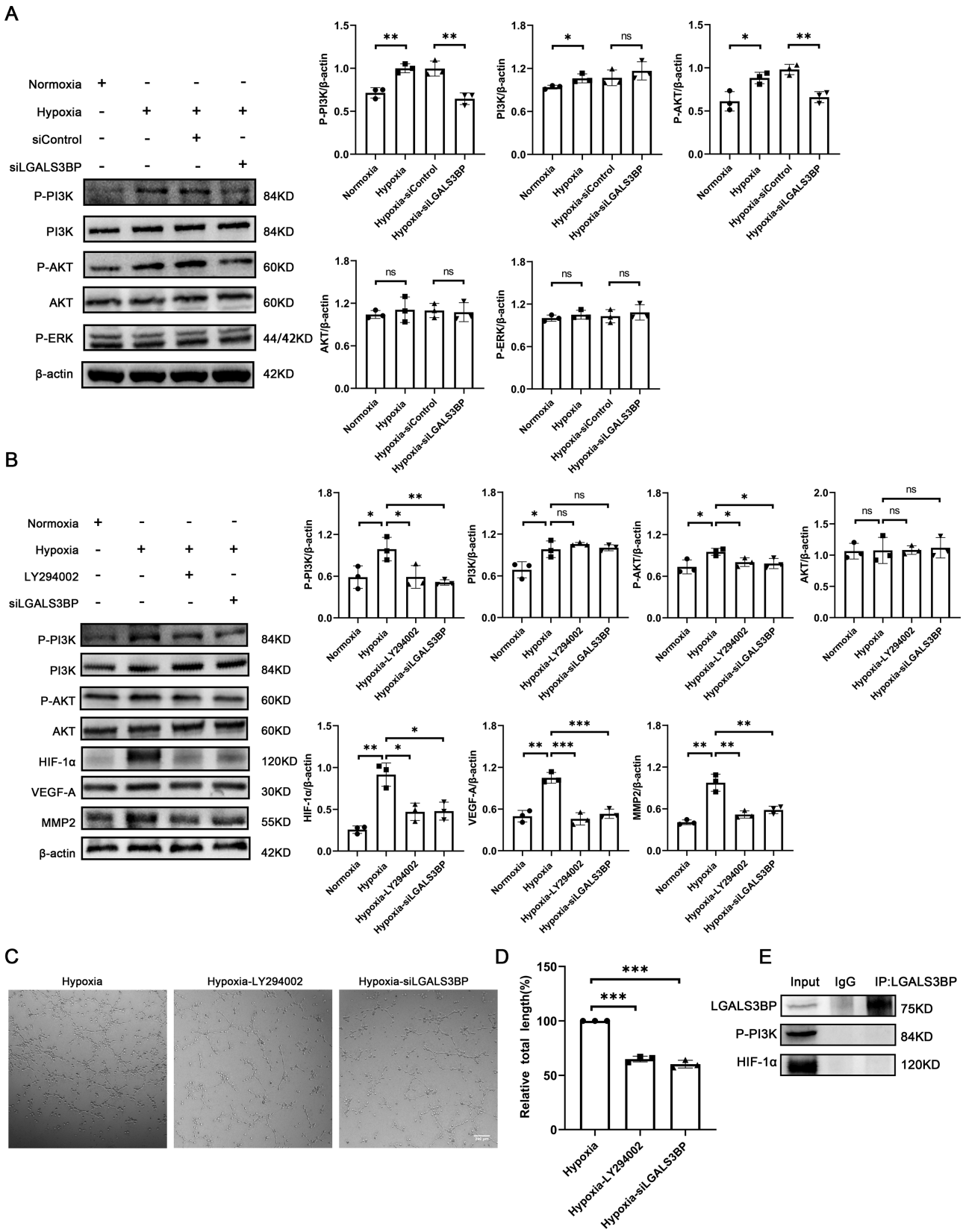

Figure 5. LGALS3BP upregulated angiogenesis-related factors through the PI3K/AKT pathway. (**A**) Representative western blotting images and quantification of phospho-PI3K, PI3K, phospho-AKT, AKT, and phosphorylated extracellular-signal regulated kinase (phospho-ERK) in LGALS3BP-silent HMC3 cells (mean ± SD; $n = 3$/group; $^{ns}P > 0.05$, $^{*}P < 0.05$, $^{**}P < 0.01$, one-way ANOVA). (**B**) The protein levels of phospho-PI3K, PI3K, phospho-AKT, AKT, HIF-1α, VEGF-A, and MMP-2 in LY294002-treated HMC3 cells (mean ± SD; $n = 3$/group; $^{ns}P > 0.05$, $^{*}P < 0.05$, $^{**}P < 0.01$; $^{***}P < 0.001$, one-way ANOVA). (**C**, **D**) Representative images and quantification of in vitro tube formation assays in Matrigel after co-culture with LY294002-treated HMC3 cells (mean ± SD; $n = 3$/group; $^{***}P < 0.001$, one-way ANOVA). *Scale bars*: 200 µm. (E) Immunoprecipitation of LGALS3BP in HMC3 cells after 24 hours of hypoxia.

Investigative Ophthalmology & Visual Science

of HIF-1α was decreased with LGALS3BP silencing. The expression levels of MMP-9, MMP-2, and VEGF-A were significantly upregulated in the HMC3 hypoxia group compared with the normoxia group, but they were also downregulated after LGALS3BP was silenced (Figs. 4A, 4B).

LGALS3BP in Microglia Regulates HUVEC Tube Formation Via the PI3K/AKT Pathway

We further investigated the mechanism by which LGALS3BP promotes the expression of proangiogenic factors in microglia and HUVEC tube formation. Previous studies have reported that LGALS3BP activates the PI3K/AKT signaling pathway to increase the expression of VEGF-A and promotes angiogenesis in endometrial cancer and breast cancer.[17] Therefore, we first analyzed the expression of PI3K and AKT and found that the phosphorylation levels of PI3K and AKT were increased during hypoxia but significantly decreased after LGALS3BP silencing. However, the total levels of AKT or PI3K were not affected regardless of hypoxia or LGALS3BP silencing (Fig. 5A). To clarify whether the PI3K/AKT signaling pathway plays a role in HUVEC tube formation, we treated HMC3 cells with LY294002, a PI3K inhibitor, during hypoxia. Our results showed that LY294002 significantly inhibited phosphorylation of PI3K and AKT, as well as angiogenic factor HIF-1α, VEGF-A, and MMP-2 in hypoxic HMC3 cells, consistent with the results for LGALS3BP-silent HMC3 cells (Fig. 5B). The treatment with LY294002 inhibited HUVEC tube formation compared with the control group (Figs. 5C, 5D). Further study was performed to elucidate the interaction between LGALS3BP and phospho-PI3K; however, we observed no direct binding between LGALS3BP and phospho-PI3K due to immunoprecipitation (Fig. 5F).

Based on the changes in HIF-1α expression shown in Figure 4 and its different roles in the molecular mechanisms of various physiological processes, we were interested in determining whether there is an interaction between HIF-1α and LGALS3BP. Immunoprecipitation showed no direct binding between HIF-1α and LGALS3BP (Fig. 5E); in fact, as shown in Figure 5, the expression of HIF-1α was obviously decreased after treatment with LY294002. These results suggest that HIF-1α is a downstream molecule regulated by LGALS3BP. In conclusion, we determined that LGALS3BP promotes the expression of angiogenic factors such as HIF-1α in HMC3 cells and tube formation of HUVECs through the PI3K/AKT signaling pathway.

Discussion

The contribution of macrophages to blood vessel formation is well recognized.[25–27] Microglia, which are derived from yolk sac primitive macrophages, also play an important role in blood vessel formation of the retina and brain.[28] The retina is populated with microglia before vascular development in rodents and humans.[10] In the developing retina, tight localization of microglia to endothelial apical cells is very important in promoting vascular sprouting.[29,30] Specifically, microglia interact with sprouting endothelial cells to facilitate anastomosis between adjacent cells.[31] The depletion of microglia (using PLX3397 or clodronate) during developmental retinal vascularization interferes with this process.[32,33]

Pathological neovascularization is a major feature of OIR,[34,35] which is mainly manifested by the rapid and massive proliferation of endothelial cells to form vascular clusters.[21,36] In our study, we found a significantly elevated LGALS3BP in the retinas of OIR mice that was positively correlated with angiogenesis, suggesting that LGALS3BP may play a proangiogenic role in the OIR model. Given these results, we knocked down LGALS3BP in HMC3 cells for relative functional and phenotypic analysis in vitro, and we further found that LGALS3BP in HMC3 cells regulates the proliferation, migration, and tube formation of HUVECs. HUVECs co-cultured with LGALS3BP-silenced HMC3 cells showed reduced ability for migration, proliferation, and tube formation, consistent with the findings of Song et al.,[17] but also reflecting the important role of microglia in promoting angiogenesis.[37,38] Previous numerous studies have shown that LGALS3BP is an important contributor to angiogenesis during tumor progression.[39,40] In addition, LGALS3BP is overexpressed in many types of cancers, and its high levels are associated with distant metastasis and poor survival in patients with a variety of cancers.[41,42] For these reasons, LGALS3BP is gradually becoming a more attractive molecule to study.

Our study found that microglia participate in angiogenesis by expressing a series of angiogenic factors, including HIF-1α, VEGF-A, MMP-2, and MMP-9, which are known to be involved in various steps of angiogenesis.[43] MMP-9 has been proven to be directly involved in the induction of tumor angiogenesis.[44] Barnett et al.[45] investigated the susceptibilities of MMP-2$^{-/-}$ and MMP-9$^{-/-}$ mice to pre-retinal neovascularization in a mouse model of OIR and found that MMP-2 plays a predominant role in retinal angiogenesis in both the mouse and rat models of OIR. HIF-1α polymerizes and nuclear translocates rapidly under hypoxia, and it combines with hypoxia-response elements of the nucleus and regulates the expression of genes involved in cellular metabolism, invasion, and angiogenesis.[46–48] In a study on neonatal retinopathy, HIF-1α increased VEGF-A expression and facilitated angiogenesis, thus accelerating disease onset and progression.[49] Similarly, in our study, the expression of HIF-1α was consistent with the expression of VEGF-A. Knockdown of LGALS3BP in HMC3 cells significantly decreased the expression of HIF-1α, VEGF-A, MMP-2, and MMP-9. We also found that HIF-1α does not directly bind to LGALS3BP by immunoprecipitation assay but belongs to the downstream molecule regulated by LGALS3BP.

We found that LGALS3BP expression levels affected PI3K and AKT phosphorylation in HMC3 cells. This suggests that LGALS3BP may regulate the expression of angiogenic factors in HMC3 cells via the PI3K/AKT signaling pathway. To further test our hypothesis, we treated cells with the PI3K inhibitor LY294002 and found that the expression of HIF-1α, VEGF-A, MMP-2, and MMP-9 was decreased, as well as the tube-forming capacity of HUVECs. This finding is consistent with the trend of knockdown of LGALS3BP. At the same time, immunoprecipitation results demonstrated that there was no direct binding between LGALS3BP and phospho-PI3K. It is well known that the PI3K/AKT signal transduction pathway is activated by several membrane receptors and plays an important regulatory function in cell survival, proliferation, and angiogenesis.[50–52] A previous study demonstrated that the PI3K/AKT signaling pathway increased the expression of VEGF-A and promoted tumor progression.[53] In addition, PI3K/AKT can also regulate the expression of genes related to matrix remolding, including

Investigative Ophthalmology & Visual Science

VEGF-A, MMP-2, and MMP-9.[54,55] Alvarez et al.[56] reported that targeting PI3K selectively inhibits retinal angiogenesis, and our study has validated these results from another perspective.

It is worth noting that the mouse model of OIR does not replicate certain aspects of ROP seen in humans.[1,57] It is a vascular wound-healing model whose application to patients with ROP is unclear because it has not been established that the clinical picture involves a vascular wound.[58,59] Although we reported that LGALS3BP in microglia could promote angiogenesis, the role of LGALS3BP in microglia in other retinal neovascular diseases remains unclear. Further studies are still needed to reveal whether LGALS3BP could play a therapeutic role in ROP disease and other retinal neovascular diseases.

In summary, we found that LGALS3BP in microglia plays an active role in angiogenesis by promoting the expression of angiogenic factors through the PI3K/AKT pathway. Our study provides the theoretical basis for therapeutic trials investigating blocking LGALS3BP-induced angiogenesis.

Acknowledgments

Supported by grants from the National Natural Science Foundation Project of China (81873678, 82070951), Natural Science Foundation Project of Chongqing (cstc2019jcyjmsxmX0120), Innovation Supporting Plan of Overseas Study of Chongqing (cx2018010), Innovative Research Group Project of Chongqing Education Commission (CXQT19015), Chongqing Education Commission (KJQN202000406), National Key Clinical Specialties Construction Program of China, Chongqing Branch of National Clinical Research Center for Ocular Diseases, Chongqing Key Laboratory of Ophthalmology (2008CA5003), and Natural Science Foundation Project of Chongqing Medical University (W0047).

Disclosure: **C. Zhao**, None; **Y. Liu**, None; **J. Meng**, None; **X. Wang**, None; **X. Liu**, None; **W. Li**, None; **Q. Zhou**, None; **J. Xiang**, None; **N. Li**, None; **S. Hou**, None

References

1. Hartnett ME, Penn JS. Mechanisms and management of retinopathy of prematurity. *N Engl J Med*. 2012;367(26):2515–2526.
2. Bashinsky AL. Retinopathy of prematurity. *N C Med J*. 2017;78(2):124–128.
3. Good WV, Early Treatment for Retinopathy of Prematurity Cooperative Group. Final results of the Early Treatment for Retinopathy of Prematurity (ETROP) randomized trial. *Trans Am Ophthalmol Soc*. 2004;102:233–248; discussion 48–50.
4. Mintz-Hittner HA, Kennedy KA, Chuang AZ, BEAT-ROP Cooperative Group. Efficacy of intravitreal bevacizumab for stage 3+ retinopathy of prematurity. *N Engl J Med*. 2011;364(7):603–615.
5. Mezu-Ndubuisi OJ, Macke EL, Kalavacherla R, et al. Long-term evaluation of retinal morphology and function in a mouse model of oxygen-induced retinopathy. *Mol Vis*. 2020;26:257–276.
6. Liu Y, Zhao C, Meng J, et al. Galectin-3 regulates microglial activation and promotes inflammation through TLR4/MyD88/NF-κB in experimental autoimmune uveitis. *Clin Immunol*. 2022;236:108939.
7. Huang Y, He J, Liang H, et al. Aryl hydrocarbon receptor regulates apoptosis and inflammation in a murine model of experimental autoimmune uveitis. *Front Immunol*. 2018;9:1713.
8. Tian Y, Zhu P, Liu S, et al. IL-4-polarized BV2 microglia cells promote angiogenesis by secreting exosomes. *Adv Clin Exp Med*. 2019;28(4):421–430.
9. Fan W, Huang W, Chen J, Li N, Mao L, Hou S. Retinal microglia: functions and diseases. *Immunology*. 2022;166(3):268–286.
10. Checchin D, Sennlaub F, Levavasseur E, Leduc M, Chemtob S. Potential role of microglia in retinal blood vessel formation. *Invest Ophthalmol Vis Sci*. 2006;47(8):3595–3602.
11. Stefater JA, 3rd, Lewkowich I, Rao S, et al. Regulation of angiogenesis by a non-canonical Wnt-Flt1 pathway in myeloid cells. *Nature*. 2011;474(7352):511–515.
12. Biswas S, Bachay G, Chu J, Hunter DD, Brunken WJ. Laminin-dependent interaction between astrocytes and microglia: a role in retinal angiogenesis. *Am J Pathol*. 2017;187(9):2112–2127.
13. Grossmann R, Stence N, Carr J, Fuller L, Waite M, Dailey ME. Juxtavascular microglia migrate along brain microvessels following activation during early postnatal development. *Glia*. 2002;37(3):229–240.
14. Silvestri B, Calderazzo F, Coppola V, et al. Differential effect on TCR:CD3 stimulation of a 90-kD glycoprotein (gp90/Mac-2BP), a member of the scavenger receptor cysteine-rich domain protein family. *Clin Exp Immunol*. 1998;113(3):394–400.
15. Resnick D, Pearson A, Krieger M. The SRCR superfamily: a family reminiscent of the Ig superfamily. *Trends Biochem Sci*. 1994;19(1):5–8.
16. Koths K, Taylor E, Halenbeck R, Casipit C, Wang A. Cloning and characterization of a human Mac-2-binding protein, a new member of the superfamily defined by the macrophage scavenger receptor cysteine-rich domain. *J Biol Chem*. 1993;268(19):14245–14249.
17. Song Y, Wang M, Tong H, et al. Plasma exosomes from endometrial cancer patients contain LGALS3BP to promote endometrial cancer progression. *Oncogene*. 2021;40(3):633–646.
18. Ullrich A, Sures I, D'Egidio M, et al. The secreted tumor-associated antigen 90K is a potent immune stimulator. *J Biol Chem*. 1994;269(28):18401–18407.
19. Piccolo E, Tinari N, D'Addario D, et al. Prognostic relevance of LGALS3BP in human colorectal carcinoma. *J Transl Med*. 2015;13:248.
20. Traini S, Piccolo E, Tinari N, et al. Inhibition of tumor growth and angiogenesis by SP-2, an anti-lectin, galactoside-binding soluble 3 binding protein (LGALS3BP) antibody. *Mol Cancer Ther*. 2014;13(4):916–925.
21. Zhou S, Zhong Z, Huang P, et al. IL-6/STAT3 induced neuron apoptosis in hypoxia by downregulating ATF6 expression. *Front Physiol*. 2021;12:729925.
22. Butturini E, Boriero D, Carcereri de Prati A, Mariotto S. STAT1 drives M1 microglia activation and neuroinflammation under hypoxia. *Arch Biochem Biophys*. 2019;669:22–30.
23. Zhang H, Zou X, Liu F. Silencing TTTY15 mitigates hypoxia-induced mitochondrial energy metabolism dysfunction and cardiomyocytes apoptosis via TTTY15/let-7i-5p and TLR3/NF-κB pathways. *Cell Signal*. 2020;76:109779.
24. Kanayasu-Toyoda T, Ishii-Watabe A, Kikuchi Y, et al. Occludin as a functional marker of vascular endothelial cells on tube-forming activity. *J Cell Physiol*. 2018;233(2):1700–1711.
25. Lingen MW. Role of leukocytes and endothelial cells in the development of angiogenesis in inflammation and wound healing. *Arch Pathol Lab Med*. 2001;125(1):67–71.
26. Sunderkotter C, Steinbrink K, Goebeler M, Bhardwaj R, Sorg C. Macrophages and angiogenesis. *J Leukoc Biol*. 1994;55(3):410–422.

27. Polverini PJ. How the extracellular matrix and macrophages contribute to angiogenesis-dependent diseases. *Eur J Cancer*. 1996;32A(14):2430–2437.
28. Unoki N, Murakami T, Nishijima K, Ogino K, van Rooijen N, Yoshimura N. SDF-1/CXCR4 contributes to the activation of tip cells and microglia in retinal angiogenesis. *Invest Ophthalmol Vis Sci*. 2010;51(7):3362–3371.
29. Gariano RF, Gardner TW. Retinal angiogenesis in development and disease. *Nature*. 2005;438(7070):960–966.
30. Rymo SF, Gerhardt H, Wolfhagen Sand F, Lang R, Uv A, Betsholtz C. A two-way communication between microglial cells and angiogenic sprouts regulates angiogenesis in aortic ring cultures. *PLoS One*. 2011;6(1):e15846.
31. Fantin A, Vieira JM, Gestri G, et al. Tissue macrophages act as cellular chaperones for vascular anastomosis downstream of VEGF-mediated endothelial tip cell induction. *Blood*. 2010;116(5):829–840.
32. Lin B, Ginsberg MD, Busto R, Dietrich WD. Sequential analysis of subacute and chronic neuronal, astrocytic and microglial alterations after transient global ischemia in rats. *Acta Neuropathol*. 1998;95(5):511–523.
33. Siren AL, McCarron R, Wang L, et al. Proinflammatory cytokine expression contributes to brain injury provoked by chronic monocyte activation. *Mol Med*. 2001;7(4):219–229.
34. Hartnett ME. Pathophysiology and mechanisms of severe retinopathy of prematurity. *Ophthalmology*. 2015;122(1):200–210.
35. Ramshekar A, Hartnett ME. Vascular endothelial growth factor signaling in models of oxygen-induced retinopathy: insights into mechanisms of pathology in retinopathy of prematurity. *Front Pediatr*. 2021;9:796143.
36. Sarigul Sezenoz A, Akkoyun I, Helvacioglu F, et al. Antiproliferative and mitochondrial protective effects of apigenin in an oxygen-induced retinopathy in vivo mouse model. *J Ocul Pharmacol Ther*. 2021;37(10):580–590.
37. Zhao X, Eyo UB, Murugan M, Wu LJ. Microglial interactions with the neurovascular system in physiology and pathology. *Dev Neurobiol*. 2018;78(6):604–617.
38. Kubota Y, Takubo K, Shimizu T, et al. M-CSF inhibition selectively targets pathological angiogenesis and lymphangiogenesis. *J Exp Med*. 2009;206(5):1089–1102.
39. Grassadonia A, Tinari N, Iurisci I, et al. 90K (Mac-2 BP) and galectins in tumor progression and metastasis. *Glycoconj J*. 2002;19(7–9):551–556.
40. Piccolo E, Tinari N, Semeraro D, et al. LGALS3BP, lectin galactoside-binding soluble 3 binding protein, induces vascular endothelial growth factor in human breast cancer cells and promotes angiogenesis. *J Mol Med (Berl)*. 2013;91(1):83–94.
41. Tinari N, Lattanzio R, Querzoli P, et al. High expression of 90K (Mac-2 BP) is associated with poor survival in node-negative breast cancer patients not receiving adjuvant systemic therapies. *Int J Cancer*. 2009;124(2):333–338.
42. Strizzi L, Muraro R, Vianale G, et al. Expression of glycoprotein 90K in human malignant pleural mesothelioma: correlation with patient survival. *J Pathol*. 2002;197(2):218–223.
43. Yin J, Xu WQ, Ye MX, et al. Up-regulated basigin-2 in microglia induced by hypoxia promotes retinal angiogenesis. *J Cell Mol Med*. 2017;21(12):3467–3480.
44. Giraudo E, Inoue M, Hanahan D. An amino-bisphosphonate targets MMP-9-expressing macrophages and angiogenesis to impair cervical carcinogenesis. *J Clin Invest*. 2004;114(5):623–633.
45. Barnett JM, McCollum GW, Fowler JA, et al. Pharmacologic and genetic manipulation of MMP-2 and -9 affects retinal neovascularization in rodent models of OIR. *Invest Ophthalmol Vis Sci*. 2007;48(2):907–915.
46. Wang GL, Semenza GL. General involvement of hypoxia-inducible factor 1 in transcriptional response to hypoxia. *Proc Natl Acad Sci USA*. 1993;90(9):4304–4308.
47. Semenza GL. Hypoxia-inducible factors: mediators of cancer progression and targets for cancer therapy. *Trends Pharmacol Sci*. 2012;33(4):207–214.
48. LaGory EL, Giaccia AJ. The ever-expanding role of HIF in tumour and stromal biology. *Nat Cell Biol*. 2016;18(4):356–365.
49. Fu Z, Chen D, Cheng H, Wang F. Hypoxia-inducible factor-1α protects cervical carcinoma cells from apoptosis induced by radiation via modulation of vascular endothelial growth factor and p53 under hypoxia. *Med Sci Monit*. 2015;21:318–325.
50. Di Y, Chen XL. Inhibition of LY294002 in retinal neovascularization *via* down-regulation the PI3K/AKT-VEGF pathway *in vivo* and *in vitro*. *Int J Ophthalmol*. 2018;11(8):1284–1289.
51. Freudlsperger C, Burnett JR, Friedman JA, Kannabiran VR, Chen Z, Van Waes C. EGFR-PI3K-AKT-mTOR signaling in head and neck squamous cell carcinomas: attractive targets for molecular-oriented therapy. *Expert Opin Ther Targets*. 2011;15(1):63–74.
52. Arcaro A. Targeting PI3K/mTOR signaling in cancer. *Front Oncol*. 2014;4:84.
53. Xu J, Yi Y, Li L, Zhang W, Wang J. Osteopontin induces vascular endothelial growth factor expression in articular cartilage through PI3K/AKT and ERK1/2 signaling. *Mol Med Rep*. 2015;12(3):4708–4712.
54. Di Y, Zhang Y, Nie Q, Chen X. CCN1/Cyr61-PI3K/AKT signaling promotes retinal neovascularization in oxygen-induced retinopathy. *Int J Mol Med*. 2015;36(6):1507–1518.
55. Wu YJ, Neoh CA, Tsao CY, Su JH, Li HH. Sinulariolide suppresses human hepatocellular carcinoma cell migration and invasion by inhibiting matrix metalloproteinase-2/-9 through MAPKs and PI3K/Akt signaling pathways. *Int J Mol Sci*. 2015;16(7):16469–16482.
56. Alvarez Y, Astudillo O, Jensen L, et al. Selective inhibition of retinal angiogenesis by targeting PI3 kinase. *PLoS One*. 2009;4(11):e7867.
57. Kim CB, D'Amore PA, Connor KM. Revisiting the mouse model of oxygen-induced retinopathy. *Eye Brain*. 2016;8:67–79.
58. Barnett JM, Yanni SE, Penn JS. The development of the rat model of retinopathy of prematurity. *Doc Ophthalmol*. 2010;120(1):3–12.
59. Rao RC, Dlouhy BJ. Mechanisms and management of retinopathy of prematurity. *N Engl J Med*. 2013;368(12):1161.

Investigative Ophthalmology & Visual Science